Short term GNSS clock characterization using One-Way carrier phase

F. Gonzalez [1,2]
[1]Geodetic Institute Karlsruhe
Karlsruhe University, Germany

P. Waller [2]
[2]RF Payload Systems Division, ESA
Noordwijk, The Netherlands

Abstract— A major effort has been done over the last years to use the carrier phase of GPS satellites signals for time transfer. Several techniques have been proposed by developing dedicated algorithms for Common View Time Transfer, Orbit and Time Network adjustments or Precise Point Positioning. Such techniques have been widely and successfully used for clock comparison and dissemination, and for the characterization of on-board clocks. In particular, GPS clocks characterization is carried out by network analysis techniques by the USNO, NRL, NGA and IGS analysis centres. It is based on the processing of GPS observables gathered over wide network of sensor stations and therefore requires complex processing of a large amount of data.

The present paper introduces a new and simple technique to characterize on-board clocks over the short term based on the carrier phase of GNSS satellites, using a single sensor station. This method uses the first derivate of the carrier phase to estimate in a simple and effective way the clock short term stability from one second. This method is successfully validated against IGS clock products for all GPS satellites, using observations from the experimental Galileo In Orbit Validation Element (GIOVE) ground network. Detailed results are presented for each GPS block clocks and signals, showing good compliance with IGS results. Results for GIOVE clock obtained with the new Galileo signals will also be presented. As shown later, this simple method equally applies for the characterization of ground clocks (receiver clocks) against the Space Clocks. In addition, it allows detailed analysis of the noise introduced by the various GNSS navigation signals.

I. INTRODUCTION

In satellite navigation onboard space clocks are a key element in the Radio Frequency chain, providing the reference frequency from which timing and signals are generated. Phase offset of the local onboard time is calculated with respect to a ground time scale reference from L-Band measurements in a least square Orbit and Time Network adjustment algorithm. This computes among other values, orbits and clock offsets for all the satellites and stations. Concerning the orbits, they are usually calculated with respect to the centre of mass assuming a fix offset to the antenna phase centre. Clocks are computed with respect to the antenna phase centre, therefore the timing signal offset computed on ground includes the hardware delay and its instability, from the signal generation to the antenna phase centre. Across the following sections this timing signal offset including the payload hardware delays and its noise will be nominated clock offset to follow the general nomenclature, although it does not refer to the physical clock. Once computed, this clock offset can be broadcasted into the navigation signal as done by the Ground Segment in the navigation message, or disseminated by other means to the user, as done by WAAS systems or IGS through its ftp service.

The timing information derived from network adjustment of orbits and clocks allows the characterization of the onboard and ground clocks. Results for GPS clocks are normally presented as the stability for one day [6],[3] since this is the nominal update rate of the navigation message or, from 5 minutes since this is the typical sample time for the network adjustment algorithms. This article presents a different approach to characterize the on board timing signal using One Way Carrier Phase Time Transfer OW-CPTT focusing on the short term behavior from 1 second.

The detailed description of the algorithm used in the OW-CPTT method is depicted in section 2. Section 3 presents the source of data used for the validation of this algorithm. Results for GPS and GIOVE-A clocks for all signal configurations are presented and discussed in section 4. Finally section 5 concludes on the benefits of this method and identifies possible improvements and further developments.

II. ALGORITHM DESCRIPTION

A. Propagation equation

The carrier phase measurement $L^i_{kj}(t)$ on the frequency k between the receiver j and the satellite i is a measurement of the beat frequency between the satellite generated frequency derived from the OB clock and the receiver generated frequency using the local oscillator or a external reference frequency. The signal propagation equation can be expressed by the following equation expressed in meters:

$$
\begin{aligned}
L^i_{kj}(t) &= \left|\left(\underline{x}^i(t-\tau^i_j)+\underline{dx}^i_k(t-\tau^i_j)\right)-\left(\underline{x}_j(t)+\underline{dx}_{kj}(t)\right)\right| \\
&+ c\left[dt^i(t-\tau^i_j)-dt_j(t)\right]+c\left[d^i_k(t-\tau^i_j)-d_{kj}(t)\right] \\
&+ I^i_{kj}(t)+T^i_j(t)+dm^i_{kj}(t)+\Delta t_r{}^i(t) \\
&+ \lambda_k N^i_{kj}+\lambda^i_{kj}\left[\phi^i_k(t_0)-\phi_{kj}(t_0)\right]
\end{aligned} \tag{1}
$$

Where each term represents:

L^i_{kj}(t) , carrier phase measurement at frequency f_k

$\underline{x}^i$, position vector of the centre of mass of the satellite in the reference system.

$\underline{x}_j$, position vector of the centre of mass of the terrestrial point in the reference system.

$\underline{dx}^i{}_k$, eccentricity vector of the transmitting antenna phase centre relative to pseudorange at frequency f_k

$\underline{dx}_{kj}$, eccentricity vector of the receiver antenna phase centre relative to pseudorange at frequency

$\tau^i{}_j$, signal travel time from the signal generator in the satellite to the signal correlator in the receiver i.e.

$$\tau^i_j = d_k{}^i + \delta\tau^i{}_j + d_{kj.}$$

dx^i_k , signal delay between signal generation in the NSGU and transmission at frequency f_k

$d\tau^i_j$, signal travel time between antennas phase centers

dx_{kj} , signal delay between the Rx antenna and signal correlation at frequency f_k

I^i_{kj} , ionospheric delay at receiver at frequency f_k

T^i_j , trospospheric delay

dt^i , satellite clock offset

dt_j , receiver clock offset

dm^i_{kj} , receiver multipath at frequency

t , receiver time at correlation instant

c , speed of light in vacuum

Δt^i_r , periodic relativistic correction due to the eccentricity of the orbit.

$\lambda_k N^i_{kj}$, integer ambiguity between the receiver and the satellite for frequency f_k at t_0

$\phi_k(t_0)$, fractional ambiguity between the receiver or the satellite for frequency f_k at t_0

Different terms can be grouped together as the geometrical distance $\rho^i_j(t)=|\underline{x}^i(t)-\underline{x}_j(t)|$ and the environmental effects $\zeta^i{}_{kj}(t)$.

$$
\begin{aligned}
L^i_{kj}(t) &= \rho^i_j(t)+\zeta^i_{kj}(t) \\
&+ c\left[dt^i(t-\tau^i_j)-dt_j(t)\right]+c\left[d^i_k(t-\tau^i_j)-d_{kj}(t)\right] \\
&+ \lambda_k N^i_{kj}+\lambda^i_{kj}\left[\phi^i_k(t_0)-\phi_{kj}(t_0)\right]
\end{aligned} \tag{2}
$$

From (2) it is possible to work out the clock phase deviation in seconds :

$$
\begin{aligned}
dt^i(t-\tau^i_j) &= dt_j(t)+c^{-1}\left[L^i_{kj}(t)-\rho^i_j-\zeta^i_{kj}(t)\right] \\
&- \left[d^i_k(t-\tau^i_j)-d_{kj}(t)\right] \\
&- c^{-1}\left[\lambda_k N^i_{kj}+\lambda^i_{kj}\left[\phi^i_k(t_0)-\phi_{kj}(t_0)\right]\right]
\end{aligned} \tag{3}
$$

B. Frequency stability

Specifications for GPS and Galileo RAFS are expressed normally in terms of Allan Deviation [3],[8]. Even if the analysis of the Hadamard deviation would be as well possible, frequency stability results will be referred to the Allan Deviation.

Time is generated from a reference frequency source, a phase deviation x(t) in the reference frequency will produce a frequency deviation. The instantaneous frequency deviation can be derived from the phase deviation for the sampling time τ_o:

$$y_k(\tau) = \frac{x(t_{k+1})-x(t_k)}{\tau} \tag{4}$$

The Allan deviation is defined not as the deviation from a mean value, but the average deviation between nearest neighbour's intervals [9].

$$\sigma^2_y(\tau_0) = \frac{1}{2}\left\langle(\Delta y)^2\right\rangle = \frac{1}{2(M-1)}\sum_{k=1}^{M-1}(y_{k+1}-y_k)^2 \tag{5}$$

Following this equations, the instantaneous frequency deviation can be obtained from the derivative of the clock phase deviation (2):

$$y^i_k(t) = d\dot{t}_j(t)+c^{-1}\dot{L}^i_{kj}(t)-c^{-1}\left[\dot{\rho}^i_j(t)+\dot{\zeta}^i_{kj}(t)\right]+\dot{d}^i_k(t-\tau^i_j)-\dot{d}_{kj}(t) \tag{6}$$

Constants terms such as the ambiguity are eliminated. The derivative of the receiver clock offset for the sampling time τ_0 represents the instantaneous receiver clock frequency offset, $y_j(t)$. Rewriting properly the above equation:

$$y^i_k(t) = y_j(t)+c^{-1}\dot{L}^i_{kj}(t)-c^{-1}\left[\dot{\rho}^i_j(t)+\dot{\zeta}^i_{kj}(t)\right] \tag{7}$$

C. Error sources

Above equation has its associated variance:

$$\sigma^{j\,2}_y(t) = \sigma^2_{y\,j}(t)+\sigma^2{}_{L}{}^i_{kj}(t)+\sigma^2{}_{\rho}{}^i_j(t)+\sigma^2{}_{\varsigma}{}^i_{kj}(t) \tag{8}$$

The higher noise among the receiver clock $\sigma^2_{yj}(t)$ and the satellite clock $\sigma^{j\,2}_j(t)$ will determine whether the satellite clock or the receiver clock is observed through the Allan deviation.

The variance associated to the carrier phase measurement of the navigation signal is expressed by $\sigma^2_{L^i_{kj}}(t)$.

The variance $\sigma^2_{\rho^i_j}(t)$ associated to the receiver-satellite distance is not purely stochastic since the estimated vector would include several residuals effects due to the inaccuracy of the different models like : receiver center of mass to receiver phase center, satellite center of mass to antenna phase center, Earth Rotation Parameters, solid earth tides, polar tides, ocean loading or wind up effect.

The higher error sources are expected to be introduced by the miss modelling of the environmental effects $\sigma^2_{\xi^i_{kj}}(t)$, like ionosphere, troposphere, periodic relativistic correction and multipath.

III. DATA SET

In order to compute the Allan deviation (5) from the equation (7) the following data are necessary: carrier phase measurements as observed by the receiver tracking, the satellite to receiver geometrical distance obtained from Satellite and Receiver coordinates in the same inertial reference frame and the physical models for correcting from deterministic errors sources as troposphere, ionosphere or periodic relativistic correction.

A. Satellite clocks and signals

Available signal from GPS and Galileo satellites are analyzed in this paper using data from the dual GPS/Galileo receiver GIOVE ground network.

Actual GPS operating blocks are Block II/IIA containing four atomic clocks: two Cesium (Cs) and two Rubidium frequency standards (RAFS) and the Block IIR containing three Rubidium atomic clocks, being the timing signal driven by the Time Keeping System. The building-up of the constellation through the demonstration phase, the completion and the on-going replenishment phase results in several clock technologies being available to the user. Enhanced RAFS (ERAFS) are foreseen for the block IIF [3] and new Cesium technologies are foreseen for the block III [4] .

Following the approval of Galileo in 1999 as a joint programme of the European Union and ESA, a demonstration element was added – the Galileo System Test Bed (GSTB) – to allow early experimentation with the navigation signals and services before committing to the final satellite design. GIOVE-A (Galileo In-Orbit Validation Element, formerly known as GSTB-V2/A) is the first of these two experimental satellites, launched on December 2005 to provide in-orbit experience for equipment which have no flight heritage, in particular the Rubidium Atomic Frequency Standard clocks (RAFS) developed by Temex Neuchatel Time (CH). GIOVE-B is scheduled at the end of 2007 and will include the Passive Hydrogen Maser (PHM) and two RAFS.

B. Receivers Ground Network.

Data from the global network of 13 Galileo Experimental Sensor Stations (GESS) is used. The networks contains Septentrio (BE) combined GPS/Galileo receivers, for time synchronization of the two systems, that collect Galileo and GPS observables at 1 Hz sampling rate.

Two GESS are connected to an external active H-masers frequency source. GIEN, located at INRiM, Turin, Italy and GUSN station located at the United States Naval Observatory, Washington, D.C. USA.. The remaining 11 stations are connected to a commercial Low Cost Portable Frequency Rubidium Standard (PFRS-01) manufactured by TEMEX-Time.

Observations from both stations connected to a H-Maser are used to analyze the satellite clocks. The remaining stations are employed to characterize the commercial clock versus the space clocks. Further description of the network, receiver , antenna and observables can be found on the GIOVE web site.**Error! Reference source not found.**

C. IGS products and SLR orbits

Currently up to eight IGS Analysis Centers (AC) contribute to earth orientation parameters and final GPS orbit and clock solutions to the IGS combinations, with centimetre accuracy. The resulting average ephemeris and clocks are output to daily files in sp3 and rinex clock formats. These products are used to provide a reference orbit to the OWCP method and to validate the stability clock results against the IGS products, the orbit is interpolated from the formal 15 minutes sampling to 1 second using a 7th order Lagrange interpolation algorithm.

For GIOVE analysis the restituted and predicted orbit calculated weekly by Satellite Laser Ranging (SLR) has been used in order to have an independent result with respect to the products provided by the Ground Processing Center (GPC). SLR is an independent high-precision technique for orbit determination based on a global network of stations that measure the round-trip flight-time of ultrashort laser pulses to satellites equipped with laser retroeflector arrays (LRAs).

For the results, obtained by the Navigation Office at the European Space Operations Centre (ESOC), for a week-based SLR only orbit determination process, the number of stations ranging GIOVE-A vary from 5 to 11 stations and amount of data accepted and rejected in the process, and the root mean square (RMS) of the residuals (the difference between the observed laser range and the estimated orbit) from 1-5 cm [5].

IV. RESULTS

In this first stage the validation is carried out without any model correction in order to verify the limits of the method and with the highest possible masking angle. Indeed, at high elevation angles, the signal to noise ratio is the highest, as the noise due to multipath and the mapping function of the environmental effects the lowest. As a result, this approach should provide the best solution. The Overlapping Allan Deviation (ADEV) is preferred to the normal Allan Deviation. For the sake of clarity in the plots the ADEV is computed at all tau values.

A. GPS clocks

Next figures present the GPS clocks separated by block and type of clock technology being operated.

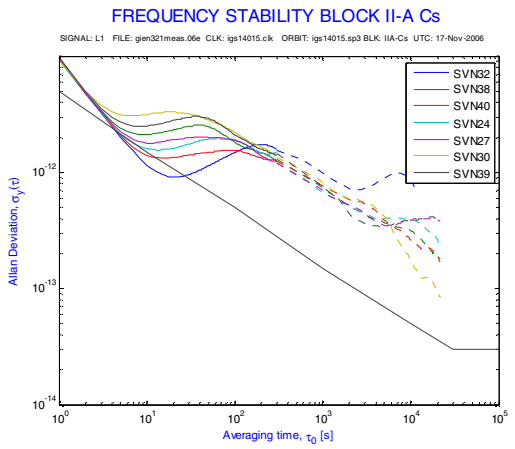

Figure 1. OWCP(L1) vs IGS, ADEV for block II-A operating a Cs

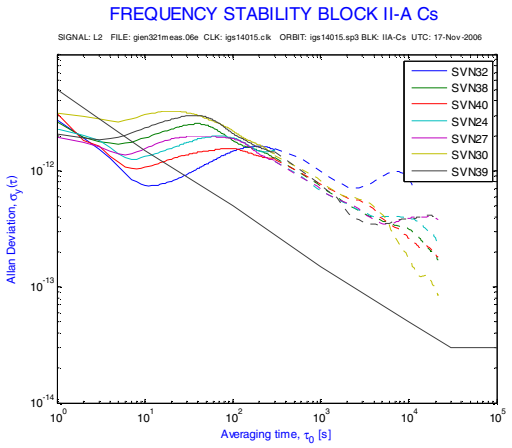

Figure 2. Figure 2 OWCP(L2) vs IGS, ADEV for block II-A operating a Cs

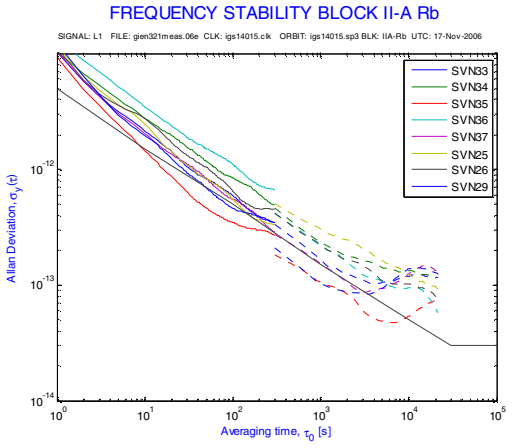

Figure 3. OWCP(L1) vs IGS, ADEV for block II-A operating a Rb

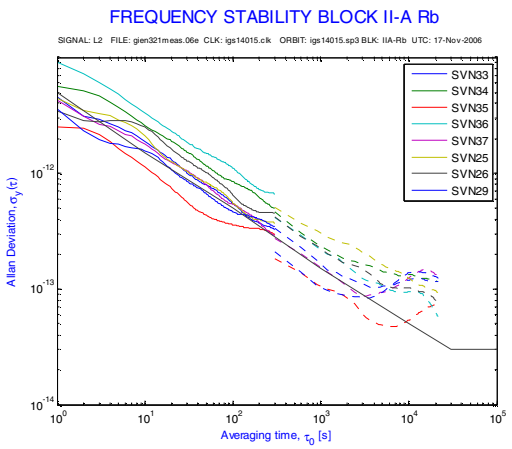

Figure 4. OWCP(L2) vs IGS, ADEV for block II-A operating a Rb

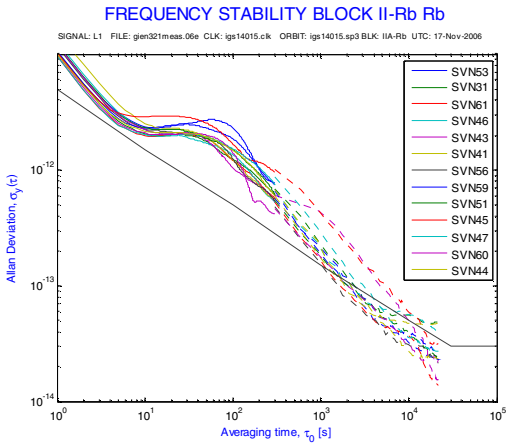

Figure 5. OWCP(L1) vs IGS, ADEV for block II-R operating a Rb

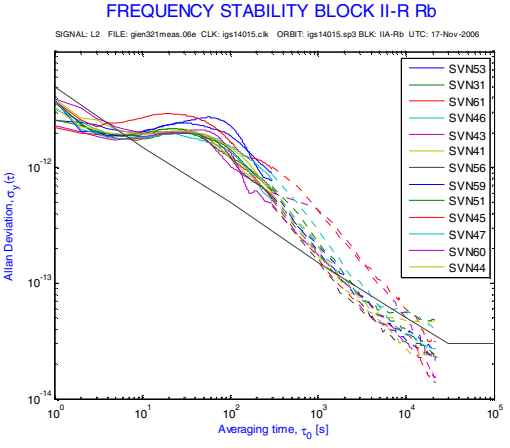

Figure 6. OWCP(L1) vs IGS, ADEV for block II-R operating a Rb

The discontinuous lines represent the clock stability obtained from IGS clock products, which is typically limited to 300 seconds sampling rate. The continuous lines present different clock stability obtained by One Way Carrier Carrier Phase estimates with GIEN station as reference with 1 second tau. For the sake of clarity the ADEV obtained from OWCP has been limited to the interval not covered by IGS products, i.e. [1,300] seconds, allowing a better visual comparison with the IGS estimates. Agreement can be verified by the noise value and slope at 300 seconds. For visual reference, the black line corresponds to $5x\ 10^{-12}\ \tau^{-1/2} + 5x10^{-14}$.On the whole the agreement between the IGS and OWCP is quite remarkable. A few satellites as PRN29 or PRN05 do not match the IGS solution at 300 seconds, however the overall trends does. Most likely the disagreement is owed to the lower elevation of the satellite which makes higher the unmodeled effects resulting in an apparent frequency drift slope.

As a general remarks, L1 and L2 results match perfectly for integration times beyond ~30sec. Below 30 seconds, L1 results are higher which clearly shows that the L1 carrier noise ($\sim 1x10^{-11}\tau^{-1}$) is masking the actual clock noise. This noise for the L1 signal would correspond to a 3 mm standard deviation. The different results between L1 an L2 below 5 seconds can be due to the smoothing algorithms employed by the semi-codeless techniques to track L2 without knowledge of the encrypted Y code.

Fig.1 and Fig.2 show a typical signature of block IIA Cesium clocks. Stability seems to be driven by an internal OCXO until it reaches a clear White Frequency Noise beyond 100 seconds ($\sim 1.2x10^{-11}\ \tau^{-1/2}$), from where it is driven by the Cs reference.

The ADEV for the block II-A Rubidium clocks (Fig. 3) present a clear White FM noise slope, in the $5x10^{-12}\ \tau^{-1/2}$ range. Best performing clock is the SVN35 ($\sim 3.5x10^{-12}\ \tau^{-1/2}$) whose ADEV is masked by the L1 noise ($1x10^{-11}\ \tau^{-1}$) until it reaches around 15 seconds.

The signal derived from the block II-R Rubidium clock (Fig. 5) presents at short term White PM noise slope from the L1 signal tracking noise. After a transition present White PM slope from around 100 seconds. Normal slope for a Rubidium Standard is White FM instead of PM, as specified in the stability specification for the PerkinElmer RAFS-IIR rubidium standard ($\sigma_y(\tau) \leq 3x10^{-12}\ \tau^{-1/2} + 5x10^{-14}$) [3]. Most likely it is due to the Time Keeping System (TKS) on board the block II-R, where a 10.23 MHz digitally controlled VCXO is linked to the RAFS by software controlled loop to produce a navigation signal with the timing accuracy of RAFS [2],.

The information about block and the operated frequency standard has been obtained from the file gpsb2.txt maintained by USNO providing information about the Block-II, and public available on the web. Although the SVN39 is marked as block II-A Rb frequency is was observed that his behavior corresponded to a Cesium standard. After further investigation this information was found inconsistent with the current status reflected in the file gpstd.txt (maintained as well by USNO) and with publications about GPS clock performance [1], where is marked as operating a Cs frequency standard.

B. *GIOVE-A clocks*

Redundant RAFS and signal generators are embarked on GIOVE-A. Flight Model FM4 is the nominal frequency source and FM5 the redundant one. All signals and the ionofree combination E5x-L1B are used to compute the OWCP solution.

Fig. 8 presents the results obtained with GUSN station, RAFS specifications and ground test results in thermal vacuum are provided as reference. The ADEV derived from the basic signals present at short term a White PM slope until the clock behavior is reached around 5 to10 seconds following onwards a White FM slope typical of Rubidium standard. From around 250 seconds the effect of the unmodeled terms becomes dominant resulting in a τ^1 slope. It is worth to remark the good adjustment between [10,300] seconds to the ground tests, $2.5\times10^{-12}\ \tau^{-1/2}$., being a key point to further validate the method.

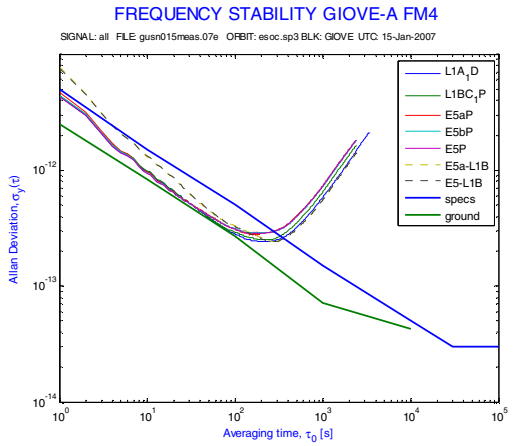

Figure 7. ADEV obtained from all signals using GUSN station for RAFS FM4 clock on board GIOVE-A

Short term noise introduced by the GIOVE navigation signals ($5\times10^{-12}\ \tau^{-1}$) is better than for GPS signals ($1x10^{-11}\ \tau^{-1}$). This validated the enhancement introduced by the new Galileo signals and codes which translates into a improved noise in the carrier phase of the navigation signals (1.5 mm). Best results are obtained with the modulation E5 ALTBOC(15,10), as expected.

Owing to the increase standard deviation after combining two signals, the ionofree combinations present a higher noise than the single signals, overwhelming the clock behavior until around 300 seconds. It is worth to mention the particular slope for the ionofree noise which does not follow a White PM or a White FM but a combination of both of them. On the other hand the ionosphere is not the main error source, since the medium term behavior linked to the τ^{-1} slope is the same as for the rest of the signals.

C. *Receiver clocks*

In case of using carrier phase observations from a station driven by a commercial oscillator, the characterized noise would be the receiver clock. As described in the equations (9), if the receiver clock variance is higher than the onboard clock,

this variance will be predominant in the Allan variance. Hence, the high quality Low Cost Portable Frequency Rubidium Standard (PFRS-01) used in the GIOVE stations different than GIEN and GUSN may be characterized using OWCP. Results can be compared to the network results obtained by the ODTS software in the Giove Processing Center.

The Allan Deviation for several GESS stations on the 2nd of March 2007 is presented on Figure 8. GESS clock specs (PFRS-01) are given as reference. RAFS specs are kept to allow for a better comparison with previous figures. The continuous line has been obtained from OWCP using E5 signal, the discontinuous lines have been obtained by the ODTS software for a 5 period day from 2nd to the 7th of March. For a better visualization only four stations are shown.

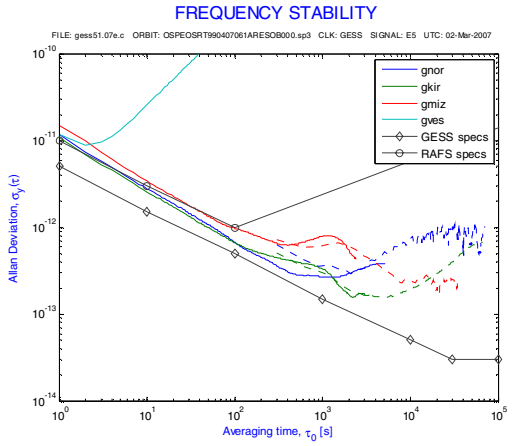

Figure 8. ADEV for several GESS stations as observed by OWCP method versus GIOVE FM5

GVES station (Vesleskarvet, Antartica) was not operating using PFRS-01 during this period and presents the typical behaviour of a crystal oscillator.

Only measurements for E5 signal during GIOVE-A passes has been used for characterize the receiver clock using OWCP while the ODTS cover 5 days. Overall agreement is quite remarkable with slightly differences most likely due to the different period covered by each method.

V. CONCLUSIONS

An initial study to verify the performance of the One Way Carrier Phase method has been presented. Allan deviation for the [1,300] seconds interval has been computed for each GPS satellite and compared against IGS results showing and overall good agreement. Results for Galileo operating clock has been compared versus the ground test matching perfectly the White FM observed on ground.

Even if further study is needed to extend the analysis to longer periods the results are quite promising. It has been show how the proposed method allows to observe the short term behavior of the space clocks from 1 second providing an independent complementary mean to network adjustment methods. These offer unquestionably better estimates at medium and long term due to the further accuracy gained by means of the physical models involved, but results are normally limited to 300 seconds sampling, imply ambiguity resolution and a difficult processing.

Similar conclusions may be drawn for the receiver clocks. Commercial PFRS-01 rubidium clocks from GESS stations have been as well characterized for their stochastic behavior, matching the ODTS results

Additionally, the method allows the characterization of the receiver carrier phase noise inherent to each broadcasted navigation signal or its combinations. For the Septentrio receiver used in the analysis the noise represents 3 mm for L1-GPS observations and 1.5 mm for Galileo signals. Results for L2 are not conclusive. This useful information may be used for characterizing the receiver or weighting properly the signals for navigation, orbit determination or time transfer purposes.

As further work, neglected physical models may be introduced in equation (8) to extend the validity of the stability analysis, additional statistic applied as the Hadamard deviation, supplementary overlapping stations driven by a H-Maser included, the new IGS clock products compared and the effect of the orbit accuracy analyzed.

ACKNOWLEDGMENT

The author would like to specially express his gratitude to Alexandre Moudrak from the Navigation Institute of the German Aerospace Agency in Oberfaffenhofen, Germany where he spent a short time in 2005 and the initial idea came out. The method was initially proposed by DLR and EADS to use carrier phase and Doppler measures to fully characterize the clock and subsequently modified by the author to focus in the carrier phase and the short term.

REFERENCES

[1] M. Epstein, “GPS IIR Rubidium Clocks: In-Orbit Performance Aspects”, in Proceedings of PTTI , 2003.

[2] J.Petzinger, R.Reith, and T.Dass. “Enhancements to the GPS Block IIR Time Keeping System” in Proceedings of PTTI , 2002.

[3] T. Dass, G. Freed, J. Petzinger, J. Rajan,T.Lynch, and J. Vaccaro. “GPS Clocks In Space: Current Performance And Plans For The Future”, in Proceedings of PTTI , 2002.

[4] R. Lutwak, D. Emmons, R. Garvey, and P. Vlitas. “Optically Pumped Cesium-beam Frequency Standard for GPS III” in Proceedings of PTTI , 2001.

[5] M.Falcone, D.Navarro-Reyes, M.Otten and M.Pearlman. “GIOVEs track: satellite laser-ranging campaigns”, GPS World . November 2006.

[6] J. Oaks, M. Largay, W. Reid, and J. Buisson “Global Positioning System Constellation Clock Performance” in Proceedings of PTTI , 2002.

[7] J. Oaks, K. Senior, M. Largay, R. Beard, and J. Buisson. “NRL Analysis of GPS On-Orbit Clocks” in Proceedings of PTTI , 2005.

[8] E.D. Kaplan C.J.Hegarty “Understanding GPS: Principles And Applications” Artech House. December 2005

[9] Allan D., “Time and Frequency (The-Domain) Characterization, Estimation, and Prediction of Precision Clocks and Oscillators” on IEEE-UFFC Transactions, Nov. 1987